TECHNICAL REVIEW

No.13 / March 2020

Technical Review
MAPNA TURBINE ENGINEERING & MANUFACTURING CO. (TUGA)

MAPNA GROUP
MAPNA TURBINE ENGINEERING AND MANUFACTURING COMPANY

Willpower to Empower Generations

Cover Page:

MAPNA Turbine Bound To Capitalize On Additive Manufacturing Technology

Editorial

Dear Colleagues, Partners and Professionals,

Providing real workable solutions that empower our clients, and working on developing and integrating new technologies in key areas that enable us to succeed hand-in-hand with our customers have ever been practiced at MAPNA Group. In this context, a brief account of a few recent achievements is presented to you, our valued readers, in this edition of MAPNA Turbine Technical Review.

The first article is a success story in dealing with premature failures typically encountered with combustor liners of the early MGT-30 industrial gas turbines. A detailed description of investigative and remedial actions taken to address the root causes of this problem and enhancing the lifetime of these critical components is presented.

As the Additive Manufacturing technology gathers more and more momentum across different industrial sectors and as it is going to play an outstanding role in our production lines in the near future, the second article introduces the recently established Additive Manufacturing Laboratory in MAPNA Turbine premises. The research center will surely serve a pioneering role in the field for the country.

The third article features development of a proficient computational code based on the Streamline Curvature Method to serve as a handy design and geometrical optimization tool by providing rapid and reliable gas flow analyses within centrifugal compressors.

Building upon successful efforts put by MAPNA Group into design, manufacturing and test of Air-cooled Condenser (ACC) gearbox, an account of which was outlined in the preceding edition of the Technical Review; the fourth article takes a more in-depth look at the vibrational analyses carried out and the measures taken to improve vibrational characteristics of these crucial pieces of power plant equipment.

Last but definitely not least, the last article reviews the meticulous steps taken to develop a calculational code and corresponding Graphical User Interface (GUI) for swift and simple calculation of stiffness coefficients in the bearings abundantly used in rotary equipment and high speed turbomachinery.

Please join us in relishing the detailed account of these subjects, in this issue of the Technical Review.

Respectfully,
Mohammad Owliya, PhD
Deputy General Director

MAPNA Turbine Company (TUGA)
March 2020

Table of Contents

03-07

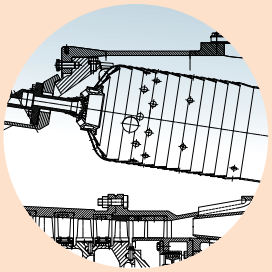

1

OPERATIONAL RESULTS OF DESIGN IMPROVEMENT ON 25 MW INDUSTRIAL GAS TURBINE COMBUSTOR

08-14

2

MAPNA TURBINE'S ADDITIVE MANUFACTURING LABORATORY

15-22

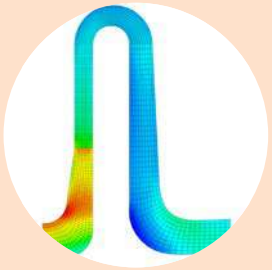

3

STREAMLINE CURVATURE METHOD IN ACTION, TO ANALYZE THE FLOW IN CENTRIFUGAL COMPRESSORS

23-30

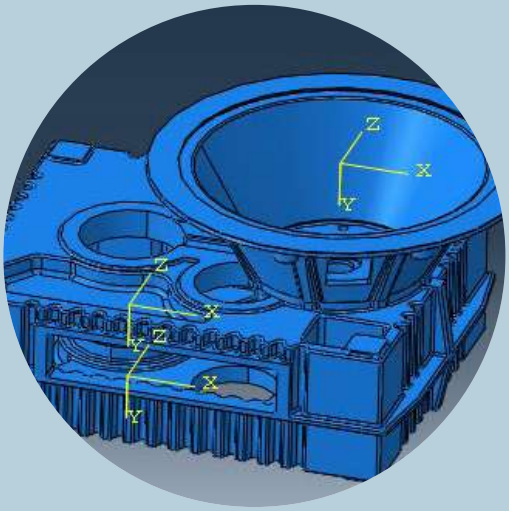

4

VIBRATION ANALYSIS OF A NEWLY DESIGNED ACC GEARBOX

31-36

5

A CODE TO SPECIFY DYNAMIC STIFFNESS COEFFICIENTS OF ROLLING BEARINGS

1

Operational Results of Design Improvement on 25 MW Industrial Gas Turbine Combustor

Introduction

Generally, one of the most important parameters in gas turbine development process is the lifetime of components, so that all users & customers could benefit from longer inspection intervals as well as minimized maintenance costs as major criteria in selecting the best suited machine. As a standard procedure, components' life time is determined based on life analysis during the design phase and is verified by product field tests later on.

In some cases failure reports prior to nominal lifetime, obtained from periodic inspections or feedbacks from users, put new limits on some components' operational life and accordingly these parts will go under design modifications and further improvements. Numerous incidents of gas turbine early defects have been reported even with well-known gas turbine OEMs. Therefore, continuous product monitoring and probable defect identification for a new gas turbine engine is obligatory and proper remedial actions should be taken to resolve the issue and rule out any early failure of product components.

According to the operational feedbacks, the early MGT-30 25 MW industrial gas turbine engine would encounter crack and oxidation on a small confined area of the liner earlier than the end of the nominal lifetime, especially for units operating close to their base-load conditions. Therefore, improvement and local modification of combustor design was performed successfully through an R&D project to eliminate the defect. By applying this modification, MGT-30 gas turbine fleet now has no serious limitation regarding the combustor components damage during the operational lifetime of the machine. Also, further increase of the liner operational life beyond the nominal value is considered to have been achieved via another development program.

Scope of Improvement

In order to investigate the combustor design characteristics of the technology transferred industrial gas turbine, a design review project was defined, looking into combustor areas of improvement. One of the most important aspects of this project was reactive numerical simulation of can-annular diffusion type combustors (Fig. 1) to determine combustor operational parameters such as air partitioning, combustor exit temperature profile and liner wall temperature distribution. According to the CFD analysis results, reduction of thermal loading in the liner in specific zones could be considered an improvement aimed to enhance its lifetime. Regarding the possible errors associated with the CFD analyses, especially on reactive flow simulation and prediction of flame structure, validation of the results using the experimental data or operational evidences is an integral part of the process. Therefore, in parallel with the progression of combustor's design review project, users' operational feedbacks on the early 25 MW gas turbine fleet as well as reports of the periodic inspections carried out on their combustors, were checked and analyzed, indicating early oxidation & overheating of liner material at almost the same positions that were predicted by the numerical simulations carried out on gas turbine units operating at higher power outputs. In other words, these damages were mostly seen in gas turbine units in which the LPT exit gas temperature and hence the net heat flux to the liner wall was higher in comparison with other units. So, based on the available evidences, numerical simulation results got validated and also, manufacturing non-conformities or any operational problems were ruled out. A photo representing damage to the liner at a critical zone is shown in Fig 2.

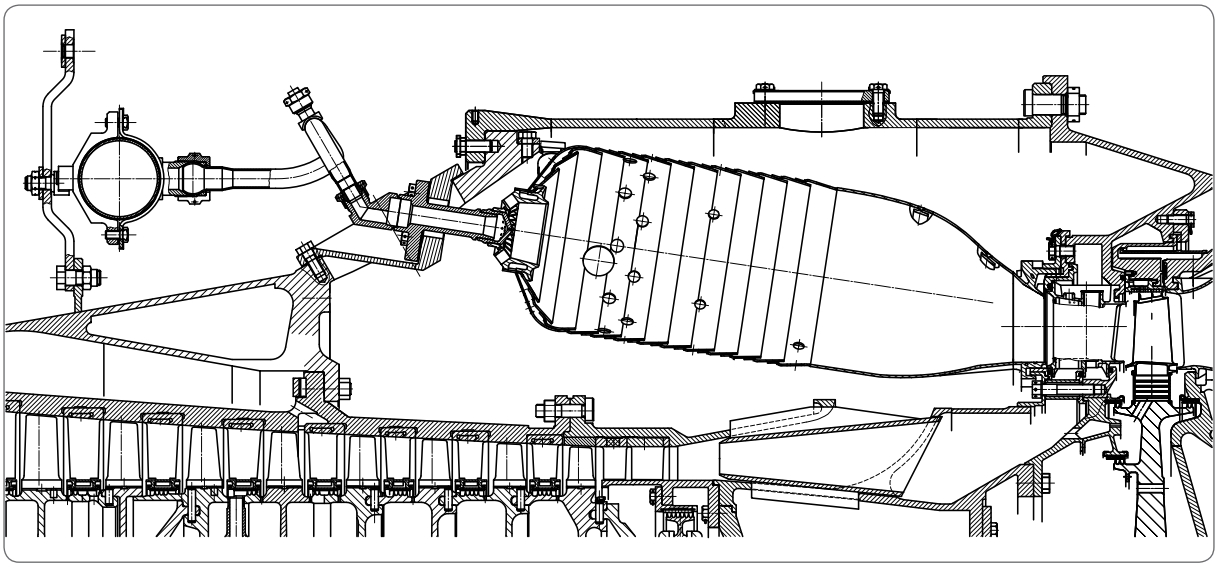

Fig. 1 – Industrial gas turbine combustor layout

Fig. 2 – Damages occurred in the combustor liner of the industrial gas turbine

As mentioned, numerical simulation results were in good agreement with operational field evidence. So, oxidation rate, as a dominant failure mechanism, was analyzed using liner material temperature obtained from CFD analyses. Comparison between liner critical zone destruction time based on oxidation rate and actual operational lifetime of the liner implies acceptable accuracy of CFD results. So, gas turbine combustion system improvement and liner wall temperature reduction at critical zones was carried out using CFD tools. This is intended to help reach the target lifetime of the component. In general, changing thermal load of the combustor's hot components could be realized via the following methods:

- Flame re-configuration by modifying fuel nozzle and air flow aerodynamic
- Improvement of the liner's cooling scheme
- Upgrading the base material & application of the thermal barrier coating layer

Of course, to choose and apply any of these methods, attention must be paid to the following constraints and considerations:

- Minimum change in combustor configuration & material which might affect manufacturing cost and complexity
- New design shouldn't involve any considerable risk in the operation of the gas turbine engine
- Regarding the possibility of failure in operating units, all project phases, including redesign, prototype manufacturing and first article testing, should be planned so as to be accomplished in minimum possible time

Finally, according to above mentioned considerations, improvement of liner cooling at critical zones was selected as the remedial action of choice.

The Industrial gas turbine combustor liner heat flux is mostly removed using film cooling mechanism in various forms at different zones and the Staked-Ring is the dominant scheme used for cooling of the cylindrical liner section. In the initial design of the combustor liner, formation of cooling air layer on damaged zones around cross fire tubes is not sufficient, resulting in locally less effective cooling. Therefore, local cooling modification needed to be carried out in such a way that air film with acceptable effectiveness is formed over critical zones, making a barrier against combustion hot gas stream and consequently, reducing the material temperature to the desired levels.

Accordingly, cooling arrangement was modified via several design verification loops, in each case cooling effectiveness and material temperature were checked using CFD tools. So, in the final design, the local liner material temperature is lowered by up to 200 °C, that based on performed lifetime analysis, It can withstand the harsh combustor conditions up to the end of the expected lifetime. The temperature distribution of the liner wall at critical zones prior and after design modifications is depicted in Fig. 3. As can be seen, the maximum local temperature is reduced about 20% around cross fire tubes in the modified liner.

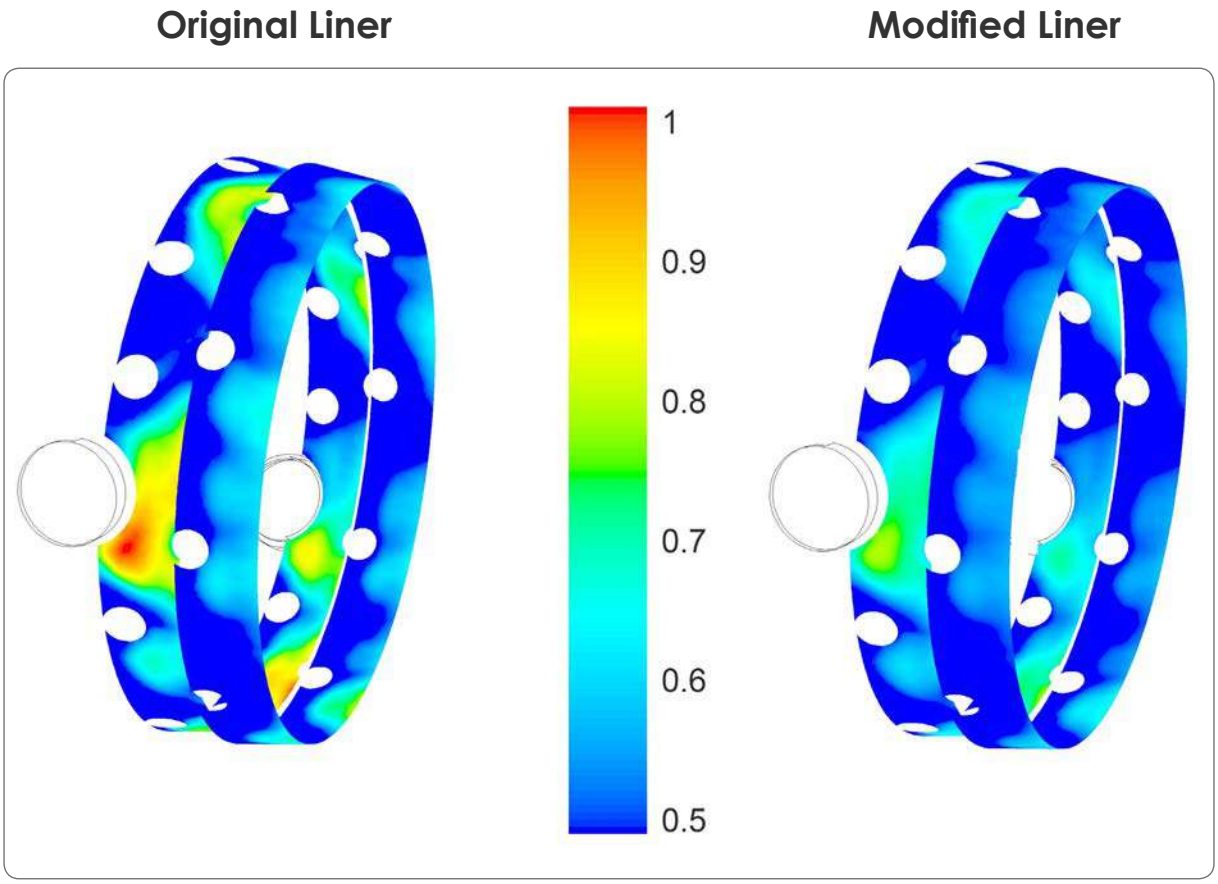

Fig. 3 – Temperature distribution contours around the critical zones of the combustor liner wall prior and after implementation of the design modifications

Prototyping and Test

In order to verify the design improvements implemented at real engine operating conditions and prior to mass production of the new liner, pilot field tests were planned on both a turbo-generator unit and a turbo-compressor set, operating at around base load conditions. It is to be noted that, by mounting the modified liners, no considerable changes in gas turbine performance characteristics were expected.

Two modified sets, each comprising 16 liners, were manufactured for the pilot units. As mentioned before, the new design was developed so that the manufacturing technology did not undergo any changes and the application of the new cooling configuration on pre-produced liners was also feasible, which was highly important from the manufacturing cost perspective.

As expected, performance parameters of both turbo-generator & turbo-compressor units equipped with the new sets of liners were completely normal and no deviation was observed in the operating parameters. Continuous inspection & planned design monitoring focused on critical modified zones in vicinity of cross fire tubes were also performed. According to the inspection data obtained from both units and up to the operating hour that local oxidation and cracks typically occurred in the liners of the original design, no sign of defect was reported and it is expected that the modified liners operational lifetime will extend up to the nominal value without any major problems given the considerable EOH accumulated by these units so far. Sample borescope photos of the modified zone at an operating hour close to the nominal lifetime of these components are shown in Fig. 4.

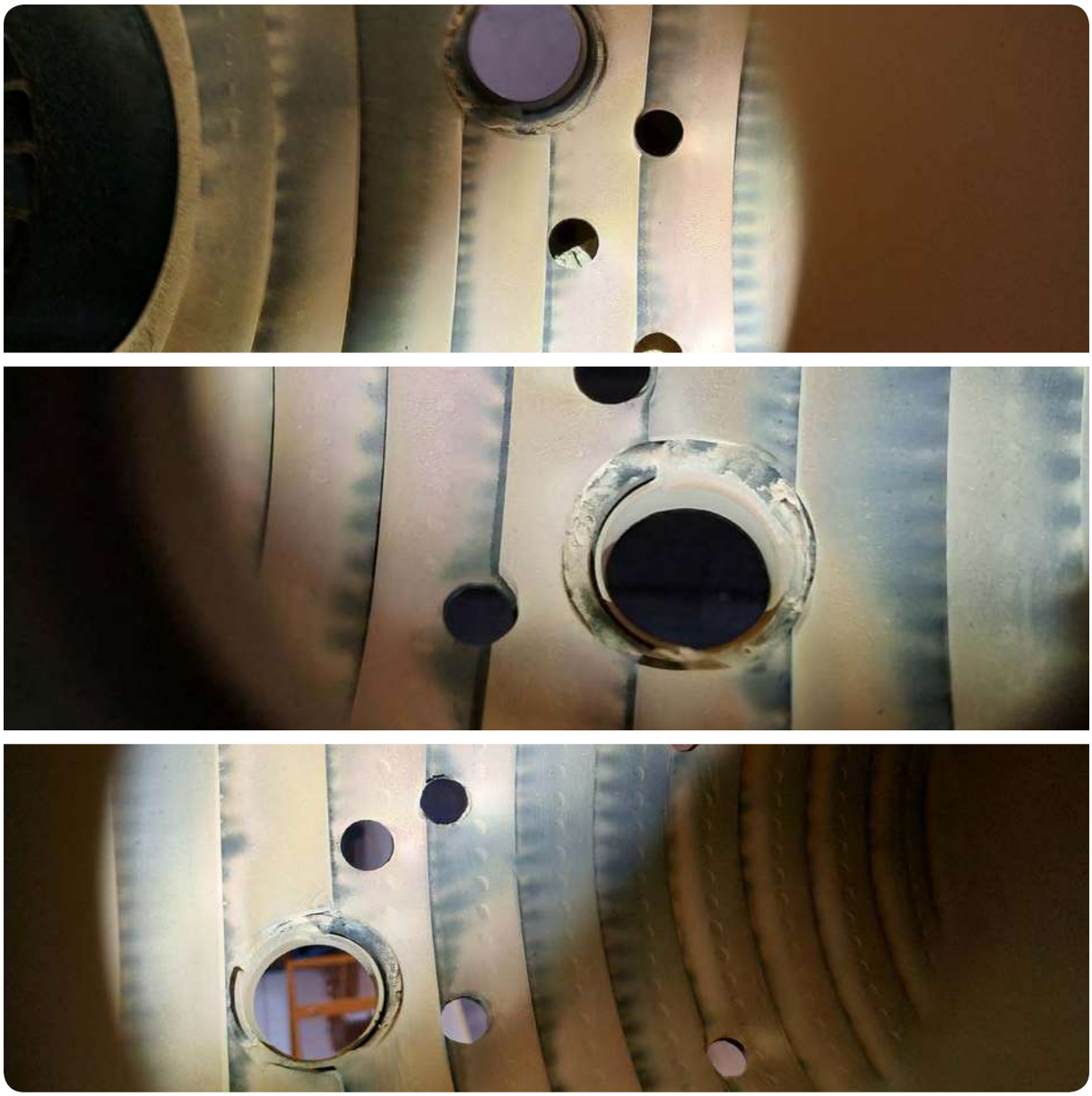

Fig. 4 – Borescope photos taken from the modified combustor liner wall at an operating hour close to the nominal lifetime of the liner

Consequently and based on successful evaluation of the modified liners, these liners are now being used in the manufacturing of the MGT-30 gas turbines and also for the operating units with higher power outputs.

A complementary R&D project is also underway regarding lifetime enhancement of the MGT-30 gas turbine liners beyond the current nominal values via further improvement of cooling scheme as well as application of TBC layers on the inner surfaces of the liners that is in the prototyping and test preparation phase.

2

MAPNA Turbine's Additive Manufacturing Laboratory

Introduction

During the past 10 years, additive manufacturing technology has altered from an attractive research concept to a reliable manufacturing process in major industries. It is playing an irreplaceable and expanding role in the field of aerospace, health care, automotive, energy and other industries. The average annual growth rate of worldwide revenue produced by all products and services is impressively 24.9%, over the course of the recent 4 years. The total metal additive manufacturing units sold in 2016 was about 980 and this value was multiplied by 235% and reached 2300 units at the end of 2018 [1]. There are a lot of interesting facts, like aforementioned ones to demonstrate that additive manufacturing is a key technology to achieve better productivity.

This added value originates from some unique aspects of the process. The additive manufacturing technology is a powerful tool for designers to design without conventional limitations. Through additive manufacturing, we can reap the benefits including but not limited to scaling down the whole supply chain and the lead time. Moreover, each part can be customized in production. Finally, prototyping will be simpler and more accessible and last, but not least, the total waste of materials is low in comparison to conventional manufacturing processes.

Inspite of all these advantages, there are several ongoing concerns toward implementation and industrialization of additive manufacturing technology. Firstly, dimensions of parts are a major limitation depending on the machine size and process characteristics. Secondly, there is not a wide range of raw materials to select as the base material. Last but not least, although the cost of machines has been reduced in recent years, most additive manufacturing processes especially metal processes are expensive. Besides, the parts usually need some post-process which increases the final cost of manufacturing.

For a reliable evaluation of the additive manufacturing technology to be implemented in a specific factory or industry, it is very important to look at the whole end-to-end process. By doing so, a reliable and realistic prediction of the final quality and cost of the parts is provided which makes it possible to gain maximum added value from the implementation of additive manufacturing technology.

Additive Manufacturing Process Chain

Selective Laser Melting (SLM) is categorized as one of the powder bed fusion (PBF) processes of metal additive manufacturing technologies [2]. It is known as the most applied and most successful technology among all metal additive manufacturing processes. Therefore, the process chain of SLM as a general process will be discussed.

As mentioned before, the process chain of an additive manufacturing process has a huge impact on both final quality and cost of a manufactured part. A typical process chain of SLM process has been shown in Fig. 1. The steps of the process can be explained as follows:

Fig. 1 – Typical SLM process chain schematic

Design: Design for additive manufacturing is a worldwide expanding concept in the field of additive manufacturing. The designers can improve the efficiency of the final product and productivity of the processes by consolidating subparts, reduction of the weight, conformal ribbing of the part casing, and applying lattice and cellular structures instead of solid parts. The design is the first and one of the most critical steps in the process chain and all subsequent activities will be performed based on it.

An example of adding value to manufacturing process of a part by consolidating subparts is shown in Fig. 2.

Data Preparation: The input data for a SLM machine shall be prepared prior to starting the process. The model shall possess a proper and optimized supports to achieve a good quality and accepted roughness of the final surfaces. Also, layering and machine parameters will be assigned to the part in this step. An adequate number of models with an optimized direction should be allocated to the building platform. This step has a significant effect on the production rate and the metallurgical and geometrical properties of the final part.

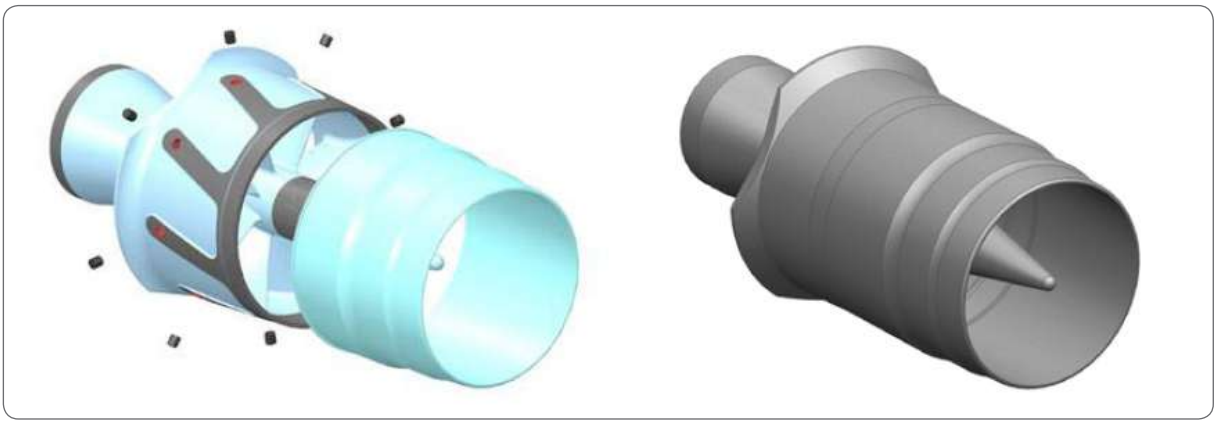

Fig. 2 – Consolidation of ten subparts forming an integrated burner swirler (Courtesy of Siemens [3])

SLM Process: If the two preceding steps are carried out properly, usually no issue will arise during the process. Of course, it should be noted that the SLM machines shall work in special conditions and various infrastructural items shall be considered. Furthermore, raw materials and their conditions are also extremely important to achieve a high quality manufactured part.

Heat Treatment: Residual stresses stemming from rapid solidification of the melt pool during the process makes it necessary to perform stress relieving heat treatment process on the part, afterwards. The residual stresses may lead to deformation of the part after separating the part from the building platform. Besides, some metallurgical phase transformations may be needed for the part to reach its final mechanical and metallurgical properties.

Support Removal: Supporting is a very complicated and crucial step during the design phase. Meanwhile, these items are temporary and should be removed from the manufactured part after separating it from the platform. It should be noted that, support removal procedure could be performed manually, mechanically (machining) and/or chemically.

Hot Isostatic Press (HIP): Generally, there are some porosities in the microstructure of the part due to layer-based nature of the SLM process and its fast solidification rate. In order to resolve this problem, HIP is an appropriate solution. HIP may be an essential step depending on the service condition of the final part.

Machining: Machining is performed generally for support removal, improving surface quality and reaching the geometrical tolerances required. It is noteworthy that, due to the complexity of the most additively manufactured parts, it is not possible to machine all surfaces. Therefore, the design shall be somehow to satisfy the geometrical tolerances of the part without any post-machining required.

Inspection: Inspection is the final step of the process chain just like any other manufacturing process. Beside all other methods, CT scan has been known as a routine method for the parts produced using SLM technology. Complexity, small size of features, small size of defects and porosities in addition to relatively inappropriate surface quality are the main reasons for utilizing this method to inspect additively manufactured parts. Also, the qualification of the process and part may be a challenge in utilizing the part for a critical application.

MAPNA Turbine Additive Manufacturing Laboratory

Considering long-term visions on manufacturing technologies and in line with the company mission as a reliable provider of turbine and compressor solutions to offer a wide range of state-of-the-art products and services to the customers, MAPNA Turbine have started a long term project to establish an additive manufacturing laboratory and develop this technology to support and complement products manufacturing processes as well as meeting the customers' requirements since 2016.

MAPNA Turbine's additive manufacturing research laboratory is designed somehow to provide A to Z knowhow, solutions and processes related to PBF methods including pre-process, manufacturing and post-process operations. At the first phase of establishing the research center, all the required infrastructures and facilities - considering the aim and scope of the center - were established and developed in a 300 m^2 area in 2019 (Fig. 3). Concisely, the target technologies for this research center are the PBF based processes of metallic materials according to the ASTM/ISO 52900 standard [2].

Fig. 3 – MAPNA Turbine additive manufacturing laboratory premises

The long term objective of our additive manufacturing center is production of parts in series to fulfil MAPNA Turbine missions and customers' requirements, and implementation of digital twin concept.

The AM Laboratory Units

- **Powder Processing**

Raw material quality is a key parameter to the final cost and respective quality of the final parts. Many of the prominent companies in the field of additive manufacturing have constituted close ties with powder production companies to guarantee the quality of their raw material and its availability. This implies the vital role of powder-oriented issues in the additive manufacturing technology especially for PBF processes in the near future. Taking this into account, the first section of the laboratory is devoted to the powder processing section. In this unit, the following activities are carried out to prepare the quality raw materials for each and every manufacturing process as well as implementing quality assurance tests for the purchased materials.

- Powder sieving
- Powder drying
- Powder properties analysis including size distribution, flowability, bulk and tap density as well as chemical analyses

- **SLM Process**

The main section of the laboratory is the SLM process section. It is equipped with two small and medium-size Noura™ machines with the following technical data.

Table 1 – SLM machines technical data

Attribute	Noura M100P	Noura M200
Building Volume [mm]	Φ125*150	Φ300*325
Laser system	Fiber laser 300W	Fiber laser 500W
Scanning speed	Up to 7.0 m/s	Up to 7.0 m/s
Focus diameter	Approx. 80µm	Approx. 80-300µm
Optic system	F-theta-lens; high speed scanner	F-theta-lens; high speed scanner

As it is clear from Table 1, the size of the building platform is specified so as to enable both research activities and the subsequent production of parts with various degrees of complexity. By doing so, nearly all designated requirements will be satisfied in the first phase. It is obvious that the number of machines could be increased in proportion to future demands. A photo representing the above-mentioned SLM machines is shown in Fig. 4.

- **Post-processing**

As mentioned earlier, post-process treatments constitute large portion of the final cost of the manufactured parts and take a great deal of attention in the process chain. According to the Wohlers report, 2019 [1], the share of post-processing activities in a metal additive manufacturing process is around 22% of the total cost of a manufactured part.

During mechanical post-processing operations, following activities are performed to improve properties of the manufactured parts, support removal as well as separating parts from the platform.

- Vibration finishing
- Electro polishing
- Machining
- EDM wire cutting
- Ultrasonic cleaning

Beside the above-mentioned post-processing operations, there are some other heating based post-processes which might be more important from the metallurgical point of view. There is also a heat-treatment section in the laboratory equipped with two muffle furnaces as well as a vacuum furnace to relieve the stresses and tailor the metallurgical microstructures of the additively manufactured parts.

Fig. 4 – Installed SLM machines at MAPNA Turbine additive manufacturing laboratory

- **Metallurgical Tests**

To ensure acceptable metallurgical and mechanical properties of a manufactured workpiece and to preform qualification tests prior and during the manufacturing process, it is essential to have a state-of-the-art metallurgical laboratory equipped with special metallurgical/ mechanical test facilities. Operating conditions including type and amount of imposed loads and service temperatures have tremendous effects on the level of qualification.

Along with the additive manufacturing laboratory, an equipped material laboratory has been established in MAPNA Turbine as well. Microstructural evaluation tests as well as mechanical properties in both ambient and high temperature environments can be performed in this laboratory. Availability of such equipment facilitates the productivity and reliability of the additive manufacturing processes.

Future Plans & Roadmap

Establishing an additive manufacturing laboratory and research center was just one initial step in the technology development process. MAPNA Group have released an additive manufacturing roadmap to become a leader in implementation of the technology.

A six-year plan based on the mentioned process chain and comprising seven headlines below has been developed and put into effect:

- Design and simulation
- Raw materials
- Additive manufacturing process
- Quality control and planning
- Validation
- Post-process
- Repeatability

According to the plan and at the end of the sixth year, the technology will have been completely developed and proven to be a reliable manufacturing process taken advantage of within MAPNA Turbine production chain. Also, the technology will be known as a tool to reduce the production time and to increase the quality of services provided for the customers.

References

[1] "Wohlers Report 2018: 3D Printing and Additive Manufacturing State of the Industry: Annual Worldwide Progress Report", *Wohlers Associates*, 2019

[2] "ISO/ASTM 52900: Standard Terminology for Additive Manufacturing–General Principles–Terminology", 2015

[3] "Redesigned for Additive Manufacturing: Serial Production of A New Fuel Swirler for Siemens Gas Turbine", *Metal AM*, 5(3): 169-72, 2019

3

Streamline Curvature Method in Action, to Analyze the Flow in Centrifugal Compressors

Introduction

The fundamental problem in the design process of a turbomachine is to specify a blade row that produces a desired energy or total pressure change given the fluid flow rate. Due to possible restrictions on size, efficiency, operating characteristics and cost of the turbomachine, additional constraints on size, speed and type of the blade row might also be necessary. The problem that a designer needs to come up with a solution to, is optimization of the blade row with respect to these constraints while still achieving the desired overall performance.

The design of a new and more efficient turbomachinery requires in-depth understanding and the ability to predict fluid flow parameters associated with the duct and blading required for the operation of such machines. In recent years, numerical methods have been developed to aid the analysis of compressible flows in compressors in both two and three dimensional simulations. Despite development of the digital computers, understanding the flow pattern and the effects of different geometric parameters on machine performance using three-dimensional analysis is not possible in short term due to complexity of the governing equations. In these cases, two-dimensional analysis is considered a viable solution.

The present study deals with the design and analysis of compressible, steady flow in turbomachinery. The basic numerical approach utilized is the Streamline Curvature Method (SCM). This method was developed more than sixty years ago in order to advance the analysis of quasi three-dimensional effects in flow through vaned and vaneless sections of a turbomachine.

Design and development of a turbomachinery would require an accurate model of the flow describing the spatial variations of the velocity and pressure in the fluid. Equations of motion are developed in a way that allows modeling of the blade row, span-wise and chord-wise load distributions on a blade row and determination of their effects on the through-flow. The related equations are solved using the SCM with the effects of turbulence taken into account empirically due to the complexity of the governing equations. The SCM was utilized to solve the design problem for blades in a cascade. Properties of the flow at the blade row inlet and exit are specified along with the loading distribution over the blade chord which is desired.

Regarding the relatively low implementation time of this method in comparison with three-dimensional CFD methods, using SCM for either comparison of different geometries or geometrical optimization provides acceptable results. Using the SCM, different designs are evaluated, leading to an optimal design as the final outcome.

The present article is the latest report on the efforts put in by MAPNA Turbine, a designer and manufacturer of centrifugal compressors, in developing state-of-the-art design software. This project has been carried out in cooperation with MAPFAN research institute in order to develop a software platform for prediction and analysis of the flow inside centrifugal compressors.

Streamline Curvature Method

In the early 1950's, Wu [1] recognized equations of motion in a turbomachinery and formulated a set of equations which had the possibility of being solved. He broke the problem of the 3D flow into a set of coupled 2D solutions. One, the meridional plane, describes the flow on hub-to-tip stream surfaces. The other, the blade-to-blade surface, describes the flow on planes generally parallel to the hub surface of the machine and perpendicular to the blading. The solutions are coupled and must be obtained iteratively to simultaneously satisfy the equations on all solution planes. Smith [2] rearranged the equations of motion in the meridional plane to give a time and spatially averaged representation of the flow in a blade row. Marsh and Katsanis [3,4] developed a solution known as the matrix through-flow method. In this method, the equations for the stream function at every grid point were solved using finite difference method, an approximation to the actual differential equations. These solutions were all basically inviscid and non-turbulent. Novak [5] formulated a SCM solution that solved for the velocities and streamlines rather than the stream functions. Davis and Millar [6] made comparisons of the usefulness of the matrix through-flow and the streamline curvature methods for through-flow predictions. They arrived at several conclusions which were important in the selection of a method for different types of problems. The advantage of the SCM developed by Novak is that the equations and solutions are in terms of physical variables of velocity and pressure rather than stream functions. Additionally, viscosity and turbulence effects were also much easier to incorporate into the SCM because their models were developed in terms of physical variables.

Given that the Novak›s writing form of equations was used in the present study, the momentum equation in the meridional plane was considered the main equation to be solved in a quasi-three-dimensional method. The prevailing assumptions were as follows:

- Steady, adiabatic, inviscid, axisymmetric flow in the meridional plane
- No volumetric forces applied

The governing equations for the streamline curvature method are as follows:

- Continuity equation
- Momentum equation (axial, radial, and circumferential)
- Energy equation
- Second law of thermodynamics
- Equations of state

In this method, instead of using the coordinates (r,θ,z), the (θ,m,n) coordinates are used, as represented in Fig. 1.

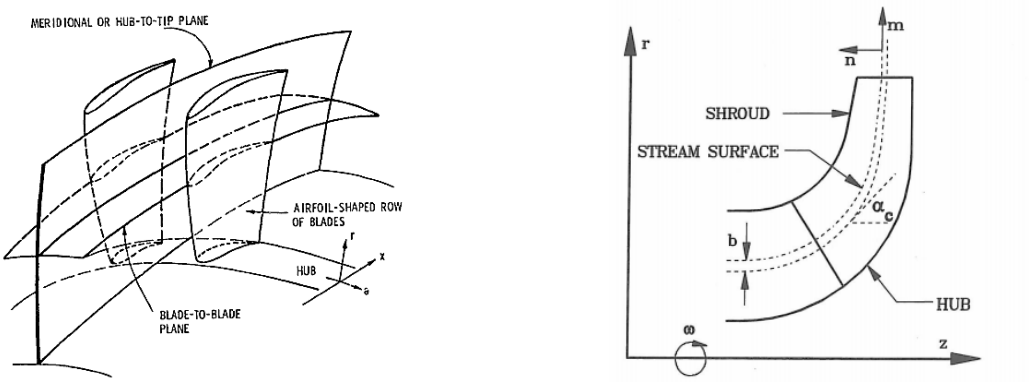

Fig. 1 – General notation of the computation planes in a turbomachinery blade row [8]

Software Development

A diagram representing modules of the developed software is shown in Fig. 2. The main part of the code comprises modules related to geometry, parts of components, mesh and solver, as denoted in Fig. 2. Thermodynamic properties of gases at different working conditions are calculated using the 'Thermodynamics' module by entering the molar percentage of different inlet gases and making use of the developed library for the physical properties of all gases.

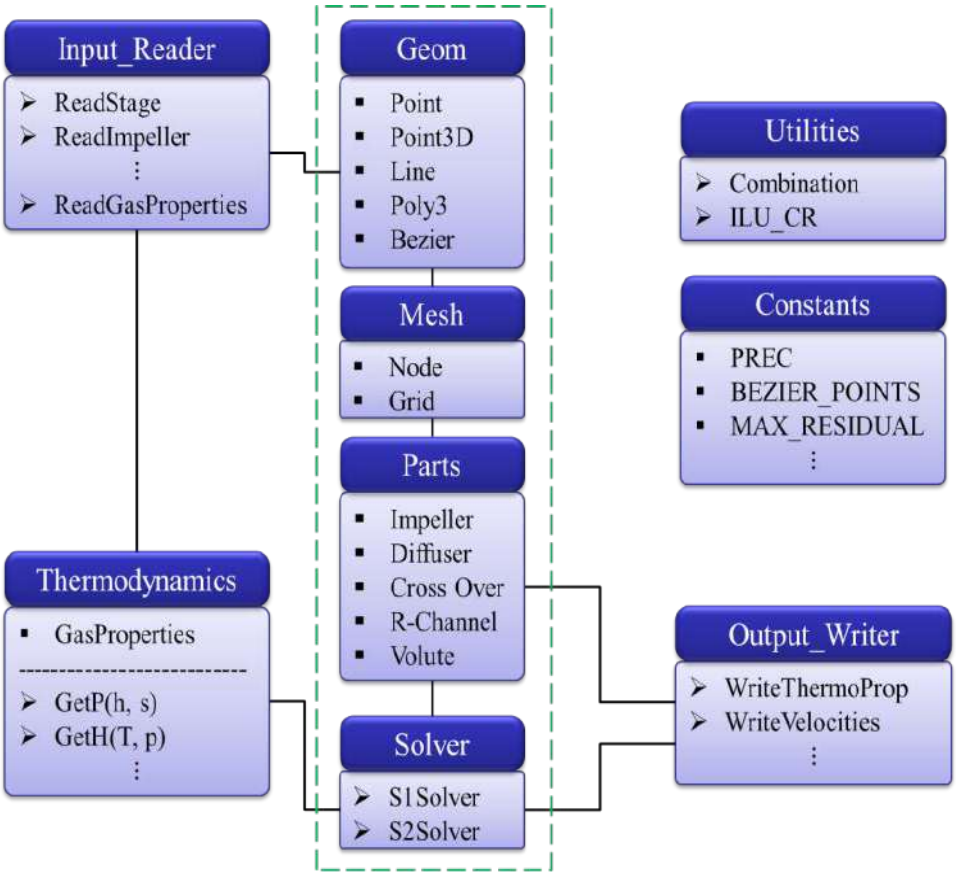

Fig. 2 – Different modules of the developed software

The first step for analysis of the quasi-three dimensional flow is to determine geometric parameters of different components and to introduce the overall geometry to the computational code. For this reason, the process of determining required parameters and entering them into the computational code is of vital importance. The fluid flow path geometry comprising the impeller, diffuser and the return bend and channel is determined making use of the Bezier method.

In accordance with the data compiled from the input file, the geometry and computational grids at hub, shroud and blade planes are produced.

To analyze centrifugal compressors, different gases are needed to be considered at different working conditions for many of which the ideal gas assumption would not apply and hence gas properties should be estimated using real gas models. So, it is necessary to have access to the thermodynamic state equations of the gases involved, i.e., thermal and caloric equations of state.

NASA's polynomial equivalence is used for ideal gas estimates in the developed software and four different methods known as Redlich-Kwong, modified Redlich-Kwong developed by Aungier [7], Soave-Redlich-kwong and Peng-Robinson›s equation are used to take into account deviations from ideal gas.

Solver modules used in the developed code, including the S1 and S2 solver modules, solve respectively the velocity potential equation on the blade-to-blade plane and governing equations on the hub-to-shroud plane.

In this method, changes of the stream functions are calculated, solving the matrix obtained from discretization of the governing equations. The general equation of stream functions is established using the continuity equation and irrotationality assumption.

In order to solve the fluid flow field in the vaned geometries such as impeller, the vaned diffuser and the return channel, it is necessary to combine the flow fields obtained on the S1 and S2 planes. For vaneless geometries such as the vaneless diffuser and the return bend, there is no need for calling the solver on the S1 plane, and the angle of streamline is considered with the assumption of angular momentum equilibrium as well as the effects of losses due to changes of the flow angle.

Results and Discussion

The accuracy of the developed numerical code for analysis of gas flow within centrifugal compressors was verified against 3D CFD simulation results, as represented in Figs. 3 and 4. As can be seen from these figures, the predicted results of the developed numerical code based on the SCM method are in good agreement with 3D CFD simulation results. However, it is to be noted that, due to some wall effects, a slight difference in the distribution of relative velocity is observed on the hub-to-shroud plane at the impeller output, implying a rather good approximation of the losses involved.

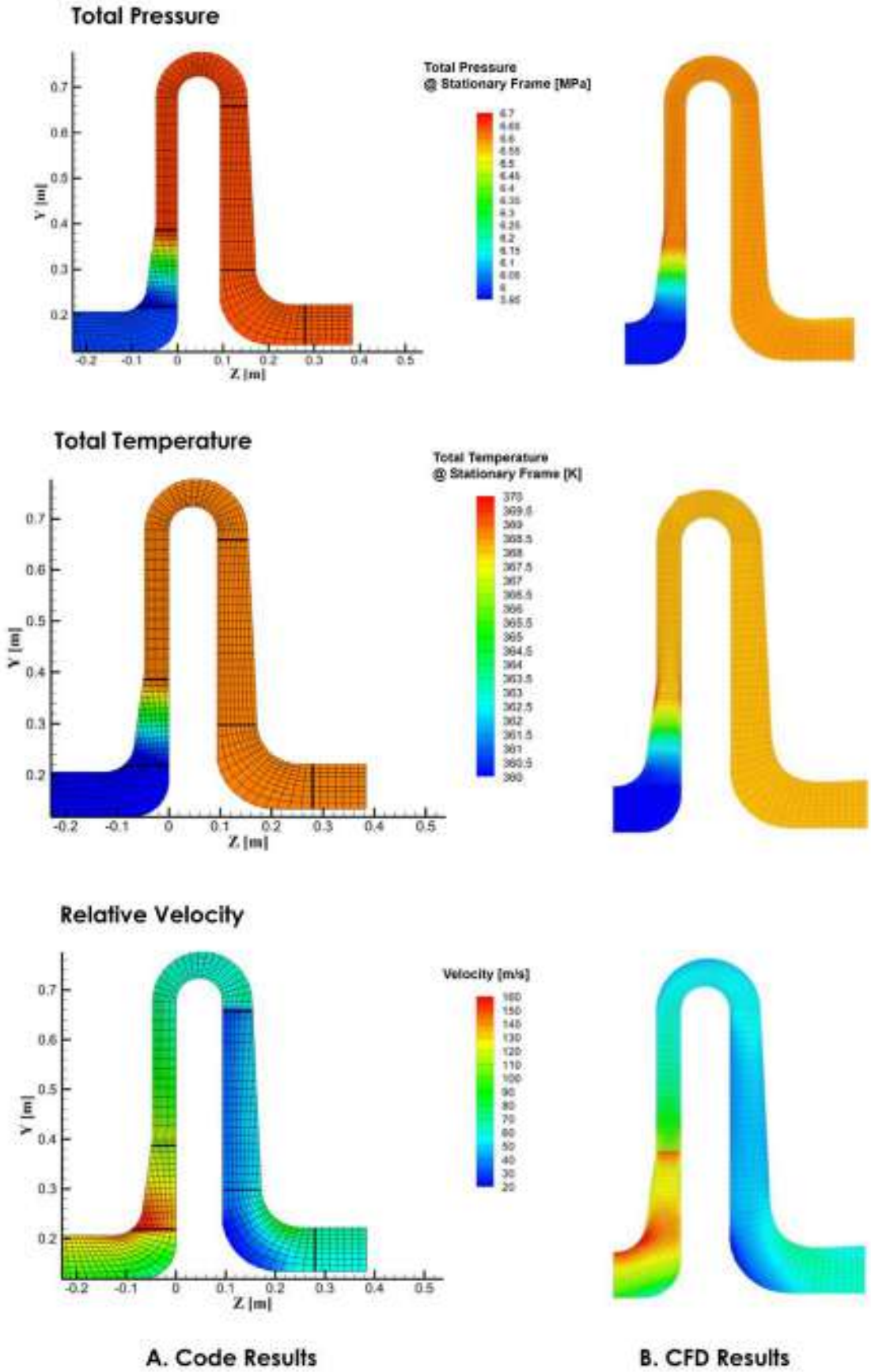

Fig. 3 – Total pressure, temperature and relative velocity distribution on the hub-to-shroud plane predicted by the developed numerical code (a) in comparison with CFD results (b)

Several compressor performance maps developed using both the SCM-based code and CFD calculations are also represented in Fig. 4, for different rotational speeds. The results are also in extremely good agreement, with a maximum discrepancy of less than 1.13% in the Pressure Ratio (PR).

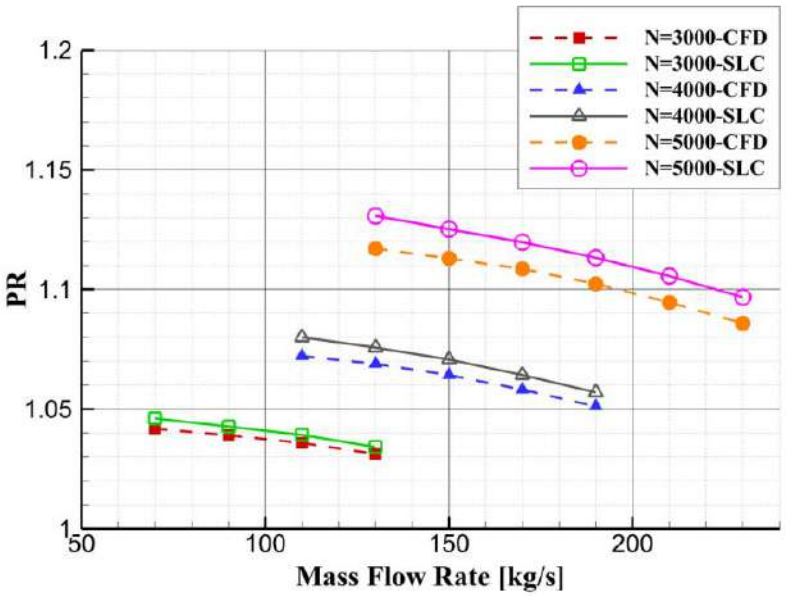

Fig. 4 – Typical compressor performance maps (PR vs. Mass Flow Rate) developed by the results of the SCM-based code and CFD calculations

A comparison of the static pressure distribution over the pressure and suction sides of a compressor blade as calculated using both the developed SCM-based code and CFD simulations is shown in Fig. 5. As it is evident in Fig. 5, the static pressure values calculated using the SCM-based code are slightly higher than those of the CFD simulations over both the pressure and suction sides of the compressor blade mainly due to losses not taken into account in the velocity potential functions.

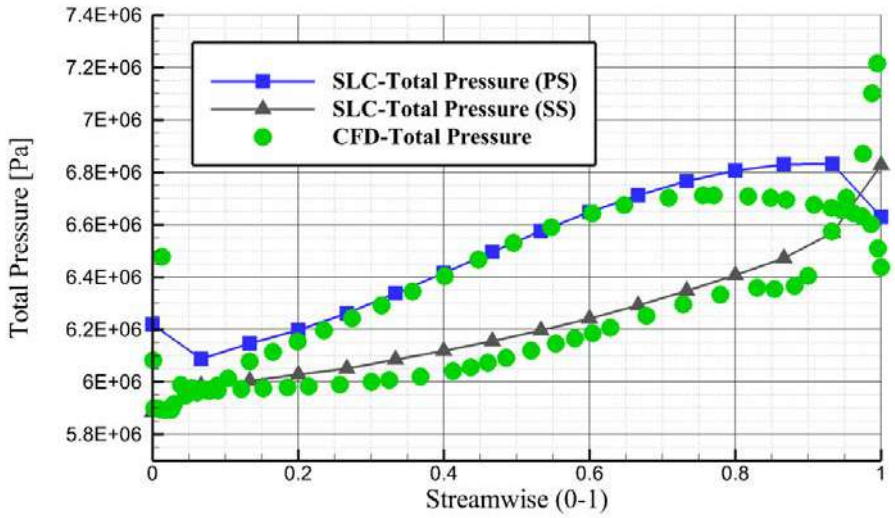

Fig. 5 – Comparison of static pressure distribution over the pressure and suction sides of a compressor blade calculated using both the SCM-based code and CFD simulations

Concluding Remarks

Developing an analytical software based on the SCM method, the gas flow inside a centrifugal compressor can be modeled and the governing equations can be solved in both the meridional (S2) and the blade-to-blade (S1) planes.

To test the validity of the in-house software developed based on the SCM method, an in-depth analysis was performed to compare the results obtained from the developed software with those from 3D CFD simulations.

According to the results, the developed computational code is shown to provide solutions in very good agreement with CFD simulations, suggesting that the tool is sufficiently accurate, especially for the preliminary design purposes.

The SCM method could be rapidly and reliably applied by a designer. Due to the complex nature of the flow between the individual blades in a cascade, the SCM method - as an analytical approach to the solution - is extremely desirable. This solution also allows the effects of each geometric and flow parameters to be determined separately. Furthermore, using the SCM method is far more efficient and agile for preliminary design and geometrical optimization purposes due to much lower execution time associated with this method in comparison with CFD simulations (approximately 20 seconds vs. 1.5 hours).

References

[1] Wu C. H., "A General Theory of Two- and Three-Dimensional Rotational Flow in Subsonic and Transonic Turbomachine", 1952

[2] Smith L. H., "The Radial-Equilibrium Equation of Turbomachinery", *J. Eng. Power*, 88: 1-12, 1966

[3] Marsh H., "A Digital Computer Program for the Through-flow Fluid Mechanics in an Arbitrary Turbomachine Using a Matrix Method", *Aeronautical Research Council*, R&M 3509, 1968

[4] Katsanis, T., "Use of Arbitrary Quasi-Orthogonals for Calculating Flow Distribution In the Meridional Plane of a Turbomachine", *NASA-TN-D-2546*, 1964

[5] Novak R. A., "Streamline Curvature Computing Procedure for Fluid Flow", *Journal of Engineering for Gas Turbines and Power*, 89: 478–90, 1967

[6] Davis, W. R., and D. A. J. Miller, "A Comparison of the Matrix and Streamline Curvature Methods of Axial Flow Turbomachinery Analysis, from a User's Point of View", *Trans. ASME, J. Eng. Power*, 1975

[7] Aungier RH, "A Fast, Accurate Real Gas Equation of State for Fluid Dynamic Analysis Applications", *J. Fluids Eng.*, 117(2): 277–81, 1995

[8] Aungier R. H., "Centrifugal Compressors: A Strategy for Aerodynamic Design and Analysis", *ASME Press*, New York, 2000

[9] Casey M. and Robinson C., "A New Streamline Curvature Throughflow Method for Radial Turbomachinery", *J. Turbomach.*, 132(3): 031021, 2010

4

Vibration Analysis of a Newly Designed ACC Gearbox

Introduction

Water supply shortages around the country have prompted power plants to consider replacing their current water-based cooling systems with Air Cooled Condensers (ACC). An ACC system comprises a supporting structure, steam ducting from the steam turbine interface, heat exchangers, finned tubes, motor gearboxes, and fans in addition to condensate and drain pumps. Smooth and reliable performance of the ACC gearboxes is instrumental in the overall performance of the ACC systems. Hiremath and Venkataram performed a dynamic analysis study on vibration characteristics of high speed gearboxes under dynamic conditions [1]. They proposed some design modifications such as changing the weight and arrangement of gears to avoid resonance. In recent years, the Finite Element Method (FEM) has widely been applied to do torsional vibration analysis of straight-geared [2] and gear-branched systems [3, 4]. Non-linear vibration of a gear pair including shaft flexibility was also simulated by Litak and Friswell [5].

An outline of the ACC system gearbox is shown in Fig. 1. The specifications of the fan and the electro-motor connected to the ACC system gearbox are also presented in Table. 1.

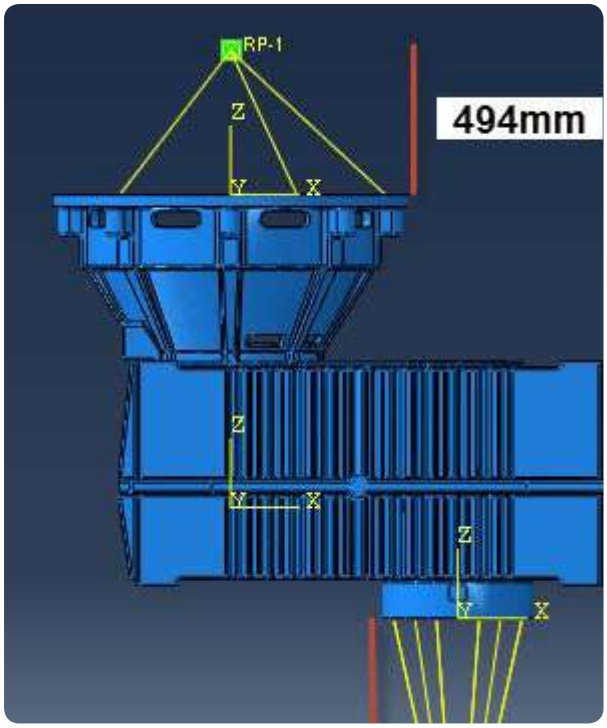

Fig. 1 – Outline of the ACC gearbox indicating location of the coupled fan and electromotor (not shown) centre of masses

It is to be noted that, ACC system gearboxes are typically designed for a long effective service lifetime of more than 20 years. The upper limits allowed for vibration and noise levels of these pieces of equipment are 3 RMS (mm/s) and 85 dB, respectively.

Table 1 – Geometrical specifications of the ACC gearbox fan and electromotor

Component	Weight [Kg]	Moment of Inertia [Kg.m^2]	Centre of Gravity [mm]
Fan	1743	30200	550
Electro motor	1580	5.6	494

Housing Vibration Analysis

The main exciting load on the housing of the gearbox is the unbalanced force applied by the electro motor which is calculated by going through different sections of the DIN ISO 21940-11 standard to determine the unbalanced class of the electromotor and the rotor weight followed by some calculational steps. The unbalanced force would be applied on electro motor's center of mass, as shown in Fig. 2.

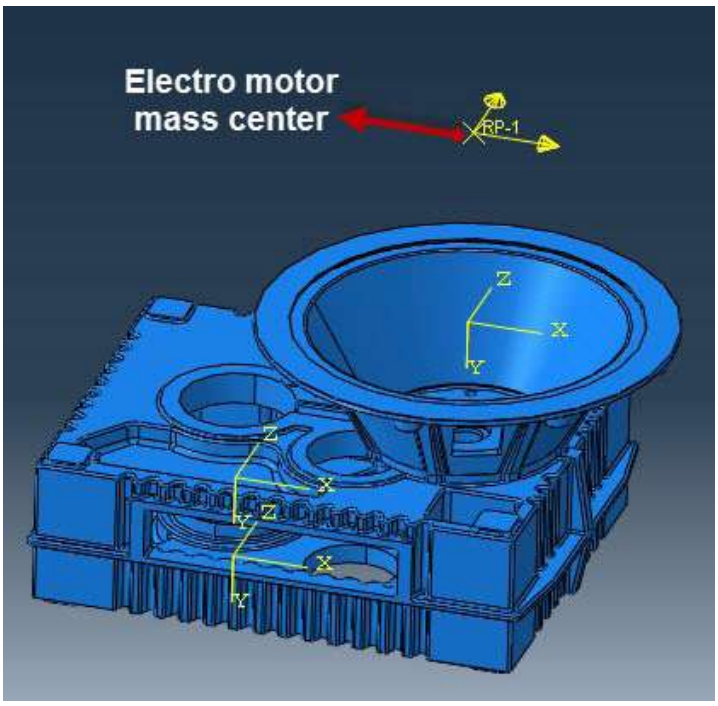

Fig. 2 – Unbalanced force applied by the electro motor on the gearbox

The unbalanced force of the ACC system fan is also obtained and accounted for using the data provided within the related catalogs.

Torsional Vibration Analysis of the Internal Components

In ACC gearboxes, the fan blade pass frequency is a potential excitation source for torsional vibrations. Torque variations occur at blade-pass frequency due to pressure disturbances resulting from blades passing a stationary object. The internal components comprise the following items:

- Flexible clutch on high speed shaft
- High speed shaft
- Pinion1 + gear1
- Intermediate shaft
- Pinion2 + gear2
- Low speed shaft

A simplified mass-spring model of the ACC gearbox internal components based on the vibrational theories [7] is shown in Fig. 3.

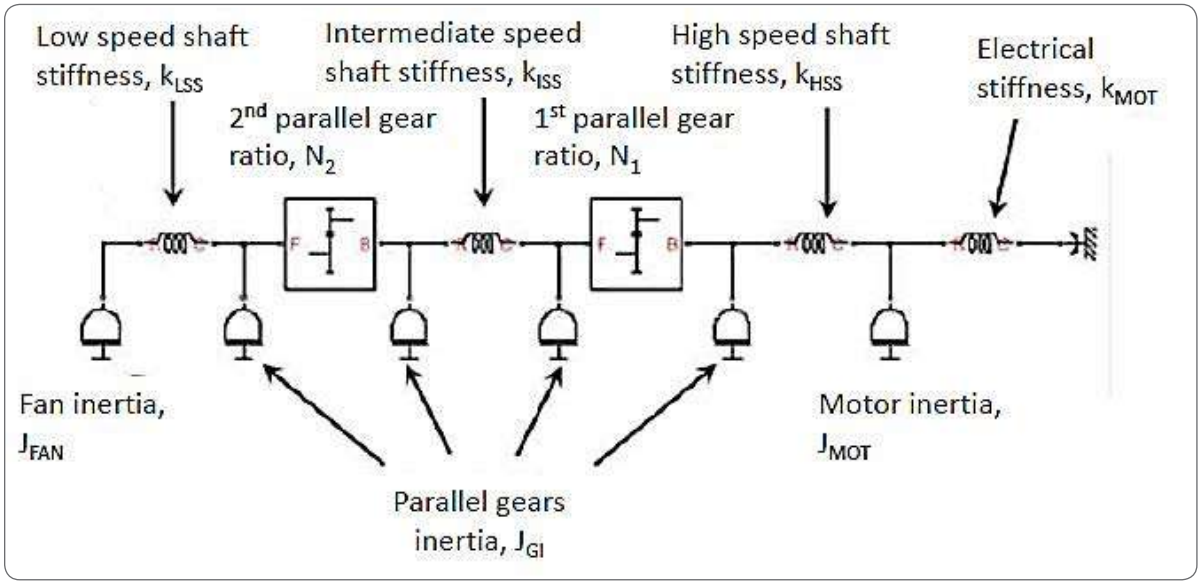

Fig. 3 – ACC gearbox internal components mass-spring model

The mass-spring model of the entire ACC gearbox system, simulated in a commercial software based on FEM method is depicted in Fig. 4.

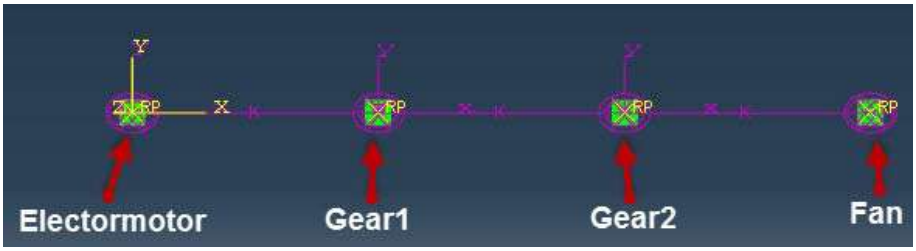

Fig. 4 – Entire ACC gearbox system mass-spring model

Results

Excitement forces applied on the ACC gearbox are listed in Table 2 in a non-dimensional format (f0 being the 10th natural mode frequency of the housing).

Table 2 – Excitement loads applied on the housing and internal components of the ACC gearbox

Excitement Loads	Non-dimensional Frequency [f/f0]
Gear Mesh Stage 1	0.75
Gear Mesh Stage 2	0.22
High Speed shaft and unbalancing force frequency due to electro motor revolution	0.043
Intermediate Shaft	0.01
Low Speed Shaft	0.002
Fan blade due to rotating blades	0.019
Blade natural frequency	0.009

The natural frequencies of the housing vibrations are listed in Table 3. Regarding the direction of the exciting force, the 4th mode shape is important and should be taken seriously. Based on experience, the directions of unbalancing force due to the electro motor is the same as the 4th mode shape of the housing, i.e., 0.061. The amount of this natural frequency should be at least 15% apart from the exciting force frequency, i.e., 0.043.

Table 3 – ACC gearbox housing natural frequencies

Mode	1	2	3	4	5	6	7	8	9	10
Non-dimensional Frequency [f/f0]	0.022	0.051	0.054	0.061	0.09	0.225	0.421	0.777	0.795	1

The frequency response of the ACC gearbox housing in the presence of the unbalanced forces in the range of 0.047-0.065 non-dimensional frequencies is illustrated in Fig. 5.

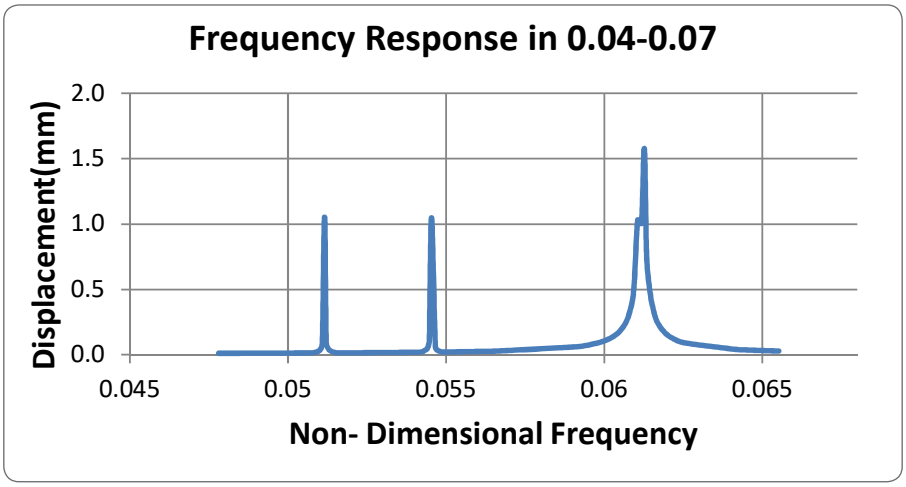

Fig. 5 – Frequency response of the ACC gearbox housing

The natural mode shape contour plots of the ACC gearbox are shown in Fig. 6 for the first four natural frequencies of vibration.

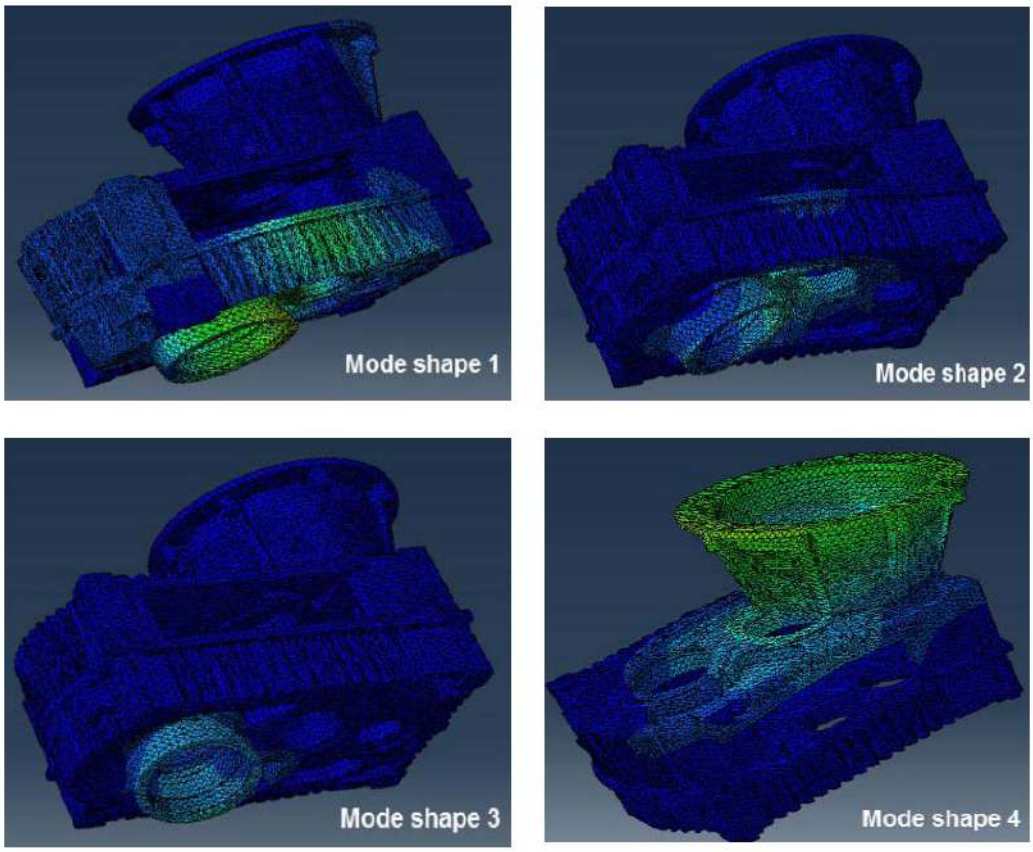

Fig. 6 – Frequency response of the ACC gearbox housing

The rotational frequency of the fan is equal to the frequency of the unbalancing force on fan which is 0.002 (Non-dimensional frequency). This value is less than the first natural frequency and also, the mode shape of the first frequency in housing is so different from the direction of the fan's unbalancing force. Therefore in this regard, unbalancing force due to fan does not have any impact on the vibrational analysis of the housing.

Torsional excitement loads on the blades of the fan (7 blades in total) could reach a huge value when one of the fan's blades is broken. The non-dimensional torsional natural frequency of the internal components is around 0.027 which is far away from the fan blade pass frequency, i.e., 0.019.

Modifications

The first step in optimization of the vibrational and acoustic characteristics of a gearbox is the gear design. The overlap contact ratio for every gear mesh shall be near to a whole number. As represented in Fig. 7, the noise levels are drastically reduced by choosing a near to whole number for the overlap contact ratio.

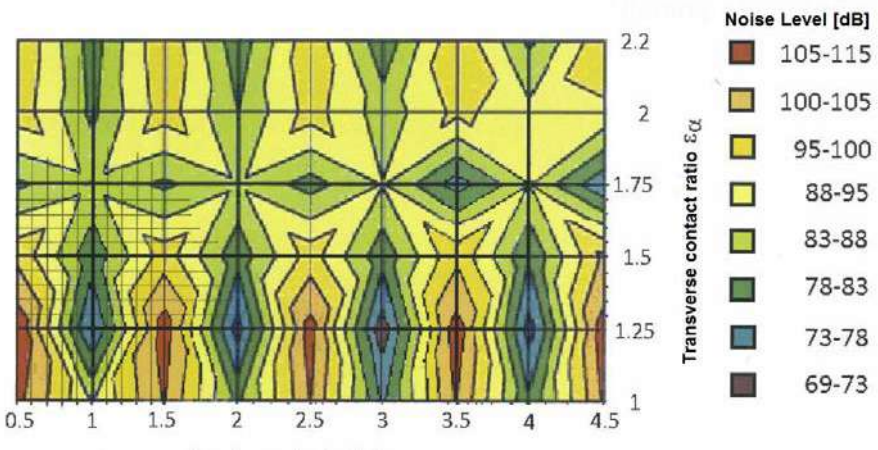

Fig. 7 – The gearbox noise level versus overlap contact ratio map

Another solution to improve the vibrational characteristics of the ACC gearbox housing was enlarging the small diameter of the gearbox lantern, specified in Fig. 8. Doing so, the 4th mode of vibration non-dimensional frequency marked in Table 3, surpassed its first mode non-dimensional frequency of 0.047.

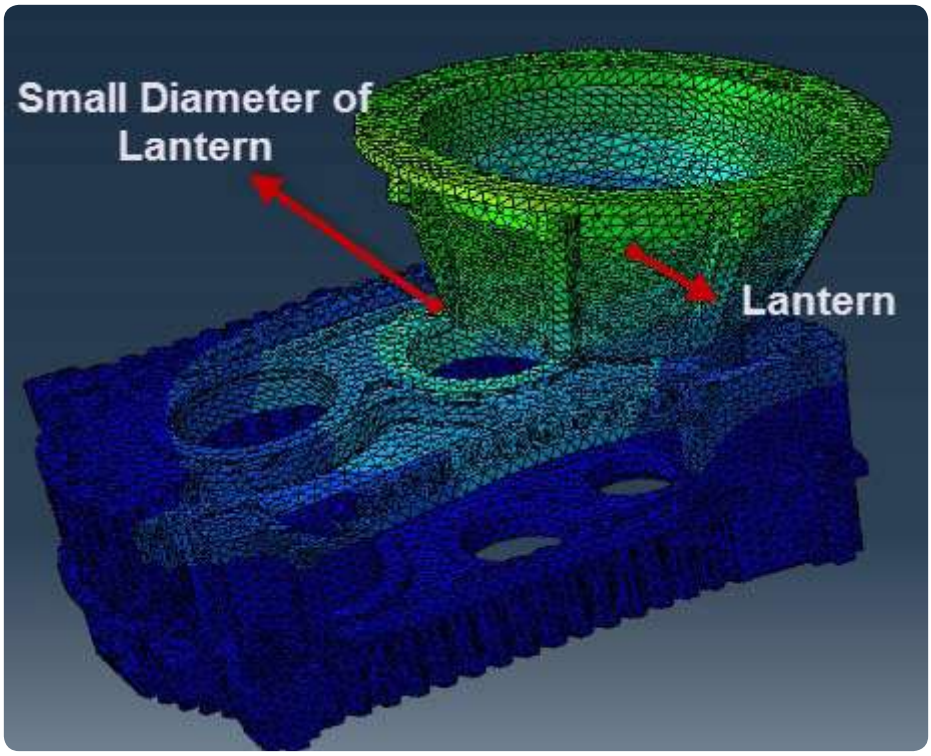

Fig. 8 – Contour plots of the ACC gearbox housing 4th mode of natural frequency

Field Tests

Manufactured brand new gearbox was finally put into operation at PARAND Combined Cycle Power Plant. Vibrations were measured at 6 critical points (2 directions each), which were the nearest points around the bearing housings, regarding natural frequencies mode shapes. These points are shown in Fig. 9.

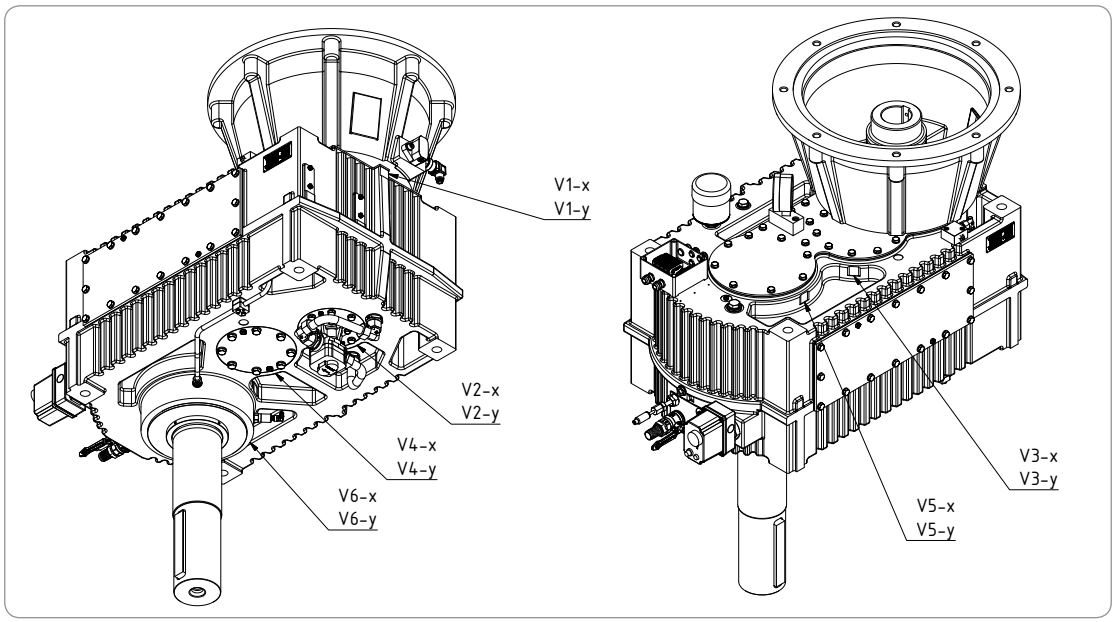

Fig. 9 – Measuring points for vibration analysis

The approach for this measurement process was running the gearbox at different rotational speeds and recording vibration values. According to the calculations, the critical speed was reached when the gearbox was running at near full speed; however, measuring was performed in a range of different values of 50%, 75%, 100%, and 110% of the nominal speed. The results are presented in Table 4.

Table 4 – Measured vibration values

Speed [rpm]	V1 mm/s		V 2 mm/s		V 3 mm/s		V 4 mm/s		V 5 mm/s		V 6 mm/s	
	X	Y	X	Y	X	Y	X	Y	X	Y	X	Y
742	0.8	0.8	1	0.9	1	1	1.1	0.8	0.9	0.9	1.1	0.8
1115	1	1	1.4	1.1	1.6	1.1	1.4	1	1.2	1.1	1.4	1
1486	1.2	2.1	2	1.6	2.2	1.8	2	2	1.3	1.6	1.9	1.9
1635	1.2	2.2	1.9	1.9	1.9	2	2.2	2.1	1.2	1.8	2.2	2.1

According to the ISO 10816 standard, acceptable vibration values at each direction shall not exceed 2.5 mm/s and as it is clear from Table 4, all recorded values were well within the acceptable range.

Concluding Note

The newly designed ACC gearbox manufactured with mentioned modifications is currently being deployed at several power plants around the country including Rudshur, Chabahr, and Urmia power plants.

References

[1] V. Hiremath and N. Venkataram., "Vibration Charecteristics of a High Speed Gearbox through Dynamic Analysis", *Materials Today*, 2017

[2] P. Schwibinger and R. Nordmann, "Torsional Vibrations In Turbogenerators Due To Network Disturbances", *Transactions of ASME*, 112, 1990

[3] H. F. Tavares and V. Prodonoff, "A New Approach for Gearbox Modeling in Finite Element Analyses of Torsional Vibration of Gear-Branched Propulsion Systems", *The Shock and vibration Bulletin*, Bulletin 56, 1986

[4] Z. LIU, S. CHEN and T. XU, "Derivatives of engenvalues for torsional vibration of geared shaft systems", *Journal of vibration and Acoustics*, 115, 1993

[5] G. Litak and M. Friswell, "Vibration in gear systems", *Chaos*, *Solitons and Fractals*, 16, 2003

[6] M. A. Corbo and S. B. Malanoski, "Practical design against torsional vibration", *Proceedings of the twenty-fifth Turbomachinery Symposium*, New York, 1996

[7] S. S. Rao, "Mechanical Vibrations", 5th Edition, Pearson, Miami, 2011

5

A Code to Specify Dynamic Stiffness Coefficients of Rolling Bearings

Introduction

Rolling bearings are one of the most common mechanical components used in different industries, especially in rotary equipment. They can be used at high radial loads and rotational speeds. This feature combined with the adaptability of these types of bearings to work at different working conditions, makes them a perfect choice for high speed gas turbines. Stiffness and damping parameters (in static and dynamic loading) are two important parameters in understanding bearing behavior and key to dynamically evaluate rotary equipment. The main purpose of this work is to calculate the stiffness of ball and roller bearings. To calculate the stiffness, the Hertzian contact will be assumed and by extracting the relationship between displacement and radial & axial loads, the equivalent stiffness is calculated. In some cases, finite element method is used to derive the stiffness, but in this research, the stiffness is calculated based on an analytical approach. Due to the variety of rolling bearings, this work includes deep groove and angular contact ball and spherical roller bearings. To verify the results, credited academic papers are utilized. Finally, a program was developed in MATLAB® with a user friendly graphical user interface (GUI).

Methodology

Loads between rotating elements (balls or rollers) and inner or outer rings in rolling bearings, are applied on only small areas of adjacent components. Even where there is only a moderate amount of force, the stress on the surfaces of the rotating elements and the neighboring ring is typically high. This stress concentration will affect calculation of stiffness. Classical equations of contact for local stress and elastic deformation, was provided by Hertz in 1896 [1]. Hertz claimed that there would be no singular point or linear contact but rather a very small area that does not let infinite stress values to emerge.

The bearing stiffness is typically a function of several different factors including mechanical properties such as modulus of elasticity, Poisson›s coefficient as well as geometrical parameters such as clearance, inner and outer diameters, etc. The bearings with radial, axial or radial-axial loads have different stiffness coefficient values.

Due to complex geometrical conditions and load distribution in the bearing elements, the stiffness of these components will be nonlinear. To calculate bearing stiffness, it is necessary to determine the local deformation at the area of contact between the rolling element and the ring according to the method proposed in [2] and [3]. To calculate stiffness, parameters such as the elastic deformation of the ball are also derived based on Timoshenko's theory and the loads that result in elastic deformation are determined using the Rajab model [4] considering several specific assumptions.

In addition to the location of the bearing components, material and geometrical parameters, rotational speed and temperature are some other important factors affecting stiffness. Generally, the inner ring temperature is higher than that in the outer ring. The temperature gradient depends on several different parameters, but its normal range is between 10 to 15 °C and the entire bearing temperature is about 30 to 50 °C more than the adjacent parts. This temperature gradient will reduce the clearance, change load distribution on rotating elements, and eventually change stiffness values. At high rotational speeds, the equilibrium position of the rolling elements, contact angles of the rotating elements and the extent of adjacent parts' engagement change and so do the bearing's radial and axial stiffness values. Utilizing the outlined procedures, stiffness coefficients are calculated and analyzed for a number of cases, of which two of the most significant ones are presented below.

1st Case Study: Deep Groove Ball Bearing

Calculations were carried out for a specific deep groove ball bearing and stiffness values for balls, rings and combination of them were calculated for different values of inner and outer raceway ring radii. The stiffness coefficient is highly dependent on the raceway radius. To obtain the equivalent stiffness value, a tangential line to the force-displacement curve was drawn as shown in Fig. 1, with its slope taken as the equivalent stiffness coefficient. The obtained equivalent stiffness coefficient for the deep groove ball bearing under investigation was in good agreement with the reference value ($K=2.3999\times10^7$ N/m) reported in the relevant literature [5].

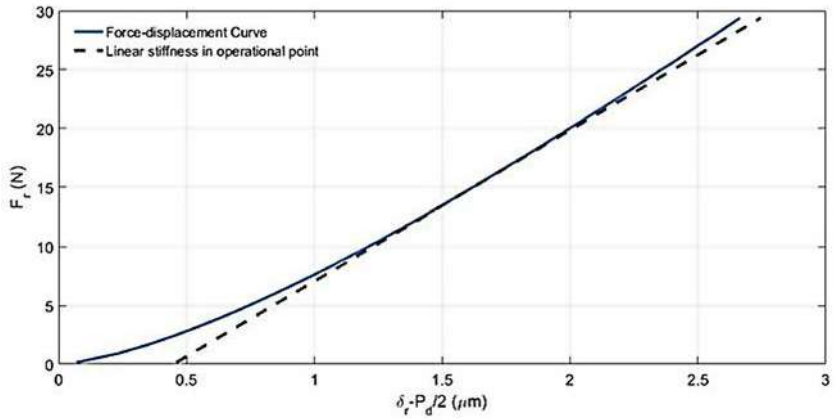

Fig. 1 – Load–Displacement diagram established for the deep groove ball bearing under investigation [5]

A diagram representing the effects of temperature difference between the inner and outer rings (0–30 °C) is presented in Fig. 2. As expected, by increasing the temperature gradient, the clearance value decreases in the range of 11 to 2 μm, and consequently the balls are much more engaged and the stiffness increases as well.

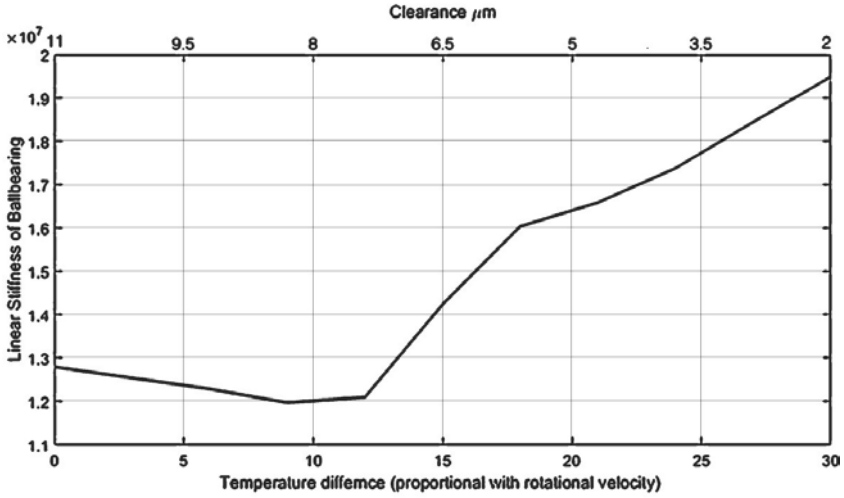

Fig. 2 – Radial deep groove ball bearing stiffness and clearance values versus the inner and outer rings temperature difference [5]

2nd Case Study: Angular–Contact Ball Bearing

For the second case, calculations were carried out for an angular-contact bearing under axial loading and the radial and axial stiffness coefficients were calculated. The stiffness versus load diagrams along with the provided reference data are presented in Figs. 3 and 4, for 300 and 9000 rpm cases, respectively. As it is obvious from Figs. 3 and 4, there is a good agreement between the calculated stiffness coefficients and the reference data provided by Sheng et al. [6].

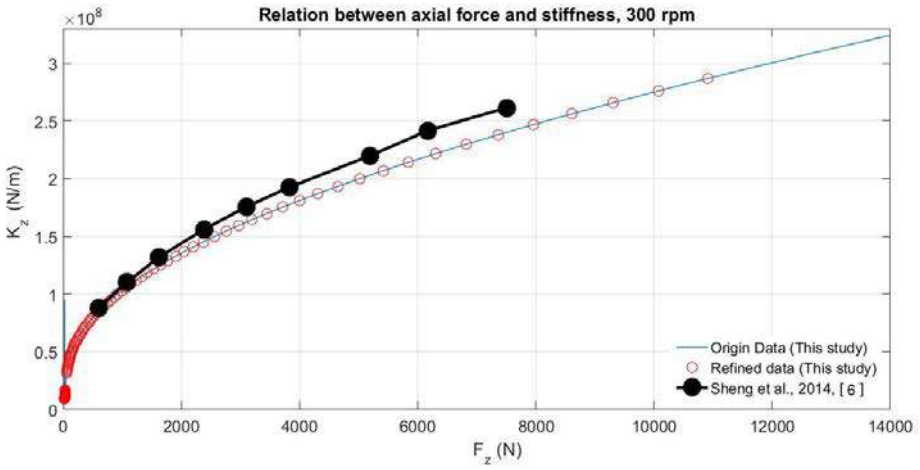

Fig. 3 – Axial stiffness versus (axial) load for angular-contact bearing at the rotational shaft speed of 300 rpm

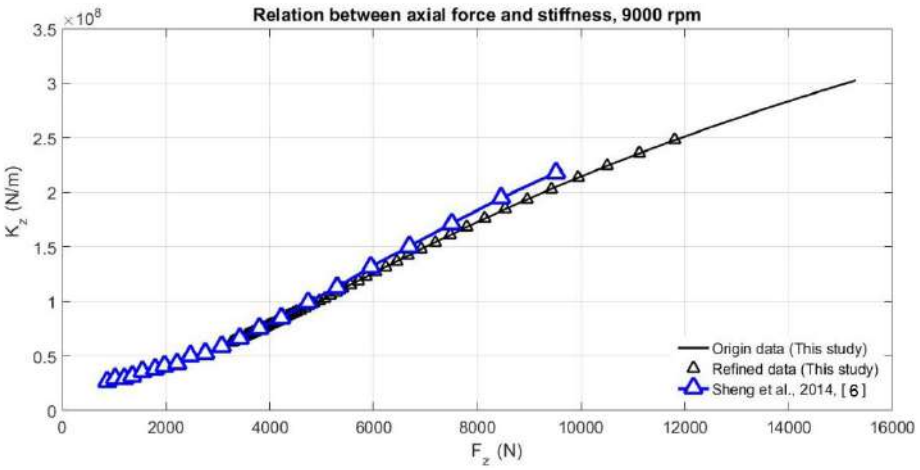

Fig. 4 – Axial stiffness versus (axial) load for angular-contact bearing at the rotational shaft speed of 9000 rpm

Developed GUI for Calculation of Stiffness Coefficients

Upon completion of the investigative analyses, a user-friendly program was written in MATLAB® to provide a robust tool for calculation of the related stiffness coefficients of different types of bearings once some specific inputs such as: type of bearing in question, type of loading applied and type of the stiffness coefficient sought(static or dynamic), are provided.

Fig. 5 shows several snapshots of the GUI developed for this purpose, representing prompts, selections and windows to select specific bearing types, specifying loading condition as well as entering bearing input parameters required to obtain the required output.

Fig. 5 – Snapshots of the GUI developed for bearings' stiffness coefficient calculation

Concluding Remarks

Calculation of stiffness coefficients in rolling bearings including deep groove and angular-contact ball bearings as well as spherical roller bearings was investigated and analyzed in a number of cases. The results provided were validated against widely cited research papers and a graphical user interface (GUI) was developed using MATLAB® to facilitate and expedite calculation of the bearings' stiffness coefficients.

References

[1] Hertz, H., "On the contact of rigid elastic solids and on hardness", *Miscellaneous Papers*, MacMillan, London, 163–183, 1896

[2] Bourgain L, Dart R, Bourgain J, "Machines tournantes et circuits pulsés. In: Applications Industrielles et médicales de l'analyse spectrale", Dunod, Edition Bordas, 392–411, 1988

[3] Shigley JE, Mitchel LD, "Mechanical Engineering Design", 4th Edition, McGraw-Hill, New York, 1983

[4] Rajab, M.D., "Modeling of the transmissibility through rolling-element bearing under radial and moment loads", PhD Thesis, Ohio State University, Colombia, Ohio, 1982

[5] Hai-lun Zhou, Gui-huo Luo, Guo Chen, Fei Wang, "Analysis of the nonlinear dynamic response of a rotor supported on ball bearings with floating-ring squeeze film dampers", *Mechanism and Machine Theory* 59: 65–77, 2013

[6] Xia Sheng, Beizhi Li, Zhouping Wu, Huyan Li, "Calculation of ball bearing speed-varying stiffness", *Mechanism and Machine Theory*, 81: 166–80, 2014

Head Office:
231 Mirdamad Ave. Tehran, I.R.Iran.
P.O.Box: 15875-5643
Tel: +98 (21) 22908581
Fax: +98 (21) 22908654

Factory:
Mapna blvd., Fardis, Karaj, I.R.Iran.
Post code: 31676-43594
Tel: +98 (26) 36630010
Fax: +98 (26) 36612734

www.mapnaturbine.com
tr@mapnaturbine.com

GR403-0